Princeton Plasma Physics Laboratory

PPPL- 4360

PPPL- 4360

Predications and Observations of Global Beta-induced Alfven-acoustic Modes in JET and NSTX

N.N. Gorlenkov, H.L. Berk, N.A. Crocker, E. Fredrickson, et. al.

October, 2008

Prepared for the U.S. Department of Energy under Contract DE-AC02-76CH03073.

Princeton Plasma Physics Laboratory
Report Disclaimers

Full Legal Disclaimer

Trademark Disclaimer

PPPL Report Availability

Princeton Plasma Physics Laboratory:

http://www.pppl.gov/techreports.cfm

Office of Scientific and Technical Information (OSTI):

http://www.osti.gov/bridge

Related Links:

U.S. Department of Energy

Office of Scientific and Technical Information

Fusion Links

IOP PUBLISHING PLASMA PHYSICS AND CONTROLLED FUSION

Plasma Phys. Control. Fusion **49** (2007) B371–B383 doi:10.1088/0741-3335/49/12B/S34

Predictions and observations of global beta-induced Alfvén–acoustic modes in JET and NSTX

N N Gorelenkov[1], H L Berk[2], N A Crocker[3], E D Fredrickson[1], S Kaye[1], S Kubota[3], H Park[1], W Peebles[3], S A Sabbagh[4], S E Sharapov[5], D Stutmat[6], K Tritz[6], F M Levinton[7], H Yuh[7], the NSTX Team and JET EFDA Contributors[8]

[1] Princeton Plasma Physics Laboratory, Princeton University, Princeton, NJ 08543, USA
[2] Institute for Fusion Studies, University of Texas, Austin, TX 78712, USA
[3] Institute of Plasma and Fusion Research, University of California, Los Angeles, CA 90095-1354, USA
[4] Department of Applied Physics, Columbia University, New York, NY 10027-6902, USA
[5] Euroatom/UKAEA Fusion Association, Culham Science Centre, Abingdon, Oxfordshire OX14 3DB, UK
[6] Department of Physics and Astronomy, Johns Hopkins University, Baltimore, MD 21218, USA
[7] Nova Photonics, One Oak Place, Princeton, NJ 08540, USA

E-mail: ngorelen@pppl.gov

Received 6 July 2007
Published 16 November 2007
Online at stacks.iop.org/PPCF/49/B371

Abstract

In this paper we report on observations and interpretations of a new class of global MHD eigenmode solutions arising in gaps in the low frequency Alfvén–acoustic continuum below the geodesic acoustic mode frequency. These modes have been just reported (Gorelenkov *et al* 2007 *Phys. Lett.* **370** 70–7) where preliminary comparisons indicate qualitative agreement between theory and experiment. Here we show a more quantitative comparison emphasizing recent NSTX experiments on the observations of the global eigenmodes, referred to as beta-induced Alfvén–acoustic eigenmodes (BAAEs), which exist near the extrema of the Alfvén–acoustic continuum. In accordance to the linear dispersion relations, the frequency of these modes may shift as the safety factor, q, profile relaxes. We show that BAAEs can be responsible for observations in JET plasmas at relatively low beta $<2\%$ as well as in NSTX plasmas at relatively high beta $>20\%$. In NSTX plasma observed magnetic activity has the same properties as predicted by theory for the mode structure and the frequency. Found numerically in NOVA simulations BAAEs are used to explain the observed properties of relatively low frequency experimental signals seen in NSTX and JET tokamaks.

(Some figures in this article are in colour only in the electronic version)

[8] See the appendix of Watkins M L *et al* 2006 *Proc. 21st Int. Conf. on Fusion Energy 2006 (Chengdu, 2006)* (Vienna: IAEA).

1. Introduction

Recently the existence of beta-induced Alfvén–acoustic eigenmodes (BAAEs) was predicted [1,2] theoretically. Initial comparisons with JET and NSTX experimental observations support the identification of low frequency magnetic activity as BAAE excitations. The shear Alfvén branch is relatively well studied especially in connection with the toroidicity-induced and reversed shear Alfvén eigenmodes (TAE and RSAE, also known as Alfvén cascades), whereas modes depending on the interaction of the fundamental Alfvén and acoustic excitations are less studied both theoretically and experimentally [3–6]. This interaction is mediated by finite pressure, plasma compressibility and geodesic curvature. As a result additional gaps in the coupled Alfvén–acoustic continuum emerge [6,7].

Recently a theoretical description of the ideal MHD Alfvén–acoustic continuum gap in the limit of low beta and high aspect ratio plasma [1] was studied. The earlier theoretical work of [6] was replicated. In addition, numerical studies found new global eigenmodes, BAAEs, and they arise near the extrema points of the continuum in both low and high beta plasmas. Experimental observations, generally qualitatively (in some cases quantitatively), support the numerical predictions of the mode frequency. Specifically, ideal MHD simulated BAAE frequency evolution qualitatively agrees with JET observations at low plasma beta of 2%, although the predicted frequency is higher by a factor of 1.77 at the maximum frequency at which these modes are observed. These calculations were based on the EFIT reconstructed q-profile. The lowest value for the frequency that ideal MHD can predict is when there is negligible ion pressure and hot thermal electrons pressure with a unity adiabatic index. There still remains the challenge of matching all the numerical predictions with the experimental results. The principal difficulty is that the predicted frequency is more than the expected experimental observations. Perhaps more accurate measurements of the q-profile can resolve the difficulty.

In NSTX with plasma beta around 20% the expected frequency seems to match the experimentally observed data, although strong toroidal rotation makes the precise frequency comparison difficult. The BAAE mode structure and the polarization data agree with the theoretical predictions within the numerical uncertainty during the flattop phase of the analyzed plasma.

In [1] it was argued that a particular value of specific heat ratio γ that was used also as kinetic effects such as due to thermal ion FLR and non-perturbative interaction with energetic particles may be responsible for the mismatch in computed and measured mode frequencies in JET. Another potential way to reconciling simulations and observation in JET is to assume that the q-profile was different from the one used in simulations. For example, the use of a slightly reversed q-profile or a higher q_0 value would be favorable for the theory–experiment comparison. In this paper we elaborate more along the lines of these arguments theoretically by studying the sensitivity of the BAAE frequency to the q-profile variation. Experimentally we present the data from the dedicated NSTX experiments, where the safety factor profile was measured with the MSE diagnostic and where good theory–experiment agreement for the mode structure and frequency (and their evolution) was observed.

The analysis of the paper is within ideal MHD theory, which is valid if the kinetic effects can be neglected such as in the case of low thermal ion temperature. Neutron measurements from JET show a much weaker neutron signal at the beginning of the discharge (when BAAEs are observed), than at a later time during the discharge when $T_\mathrm{i} \simeq T_\mathrm{e}$ was measured. This indicates that at the time of BAAE observations the assumption of $T_\mathrm{i} < T_\mathrm{e}$ can be made and the kinetic effects due to ion FLR can be neglected. However, in NSTX plasma measurements show that $T_\mathrm{i} \simeq T_\mathrm{e}$ and for the proper treatment of the problem one has to evaluate the kinetic

effect. We will consider such effects in future publications and will focus in this paper on how well ideal MHD can describe low frequency observations in JET and in NSTX. Ideal MHD results also can be useful as model results and produce limit cases for the kinetic theories.

We note that by understanding the range of BAAE frequency excitation and observing or exciting these frequencies in experiments we may be able to potentially extend the use of MHD to determine q_0 (and/or $q_{\min}$). Such observations could be a very important diagnostic tool for ITER and other burning plasma experiments. This observation would also help to infer the central plasma beta and the ion and electron temperatures.

The paper is organized as follows. In section 2 we outline the derivation of the Alfvén–acoustic continuum and its extrema points and the frequency gap. We apply theory and NOVA simulations to JET and NSTX plasmas in sections 3 and 4, respectively. The summary is given in section 5.

2. Low frequency Alfvén–acoustic continuum

Here we outline the theory of the ideal MHD continuum presented in [1], where a limit case of a low beta, high aspect ratio plasma was analyzed in details in order to derive the dispersion relation of the low frequency Alfvén–acoustic continuum. The plasma compressibility effect includes the specific heat ratio, γ. It was obtained that at $\delta \equiv \gamma\beta/2 \ll 1$ the frequency of the continuum satisfies the equation similarly to the one obtained in [6]:

$$(\Omega^2 - k_0^2/\delta)(\Omega^2 - k_{+1}^2)(\Omega^2 - k_{-1}^2) = \Omega^2(2\Omega^2 - k_{+1}^2 - k_{-1}^2), \tag{1}$$

where the frequency is normalized $\Omega^2 \equiv (\omega R_0/v_A)^2/\delta$, R_0 is the major radius of the torus, v_A is the Alfvén velocity and we denoted parallel wavevectors of different poloidal harmonics of the perturbed quantities as $k_j = (m + j - nq)/q$, where m and n are the poloidal and toroidal mode numbers. The oscillations of an infinite medium, the two acoustic modes $\Omega^2 = k_{\pm 1}^2$ and the shear Alfvén wave $\Omega^2 = k_0^2/\delta$ (valid if condition $k_0^2/\delta \gg 1/q_r^2$ is satisfied), in the absence of toroidal effects are described by this dispersion if the left-hand side is set to zero, that is when the coupling effect from the geodesic curvature is neglected. Note, that we used a more general condition (arbitrary q) instead of $k_0^2/\delta \gg 1$ from [1] (for q not far from unity).

In the vicinity of the rational surface, $q_r = m/n$, we find from equation (1) in the limit $k_0^2/\delta \ll 1$ two low frequency roots. One root is

$$\Omega^2 = 1/q^2 \tag{2}$$

and the second solution with a much lower frequency was called the modified shear Alfvén wave

$$\Omega^2 = k_0^2/\delta(1 + 2q^2). \tag{3}$$

We note that at a higher frequency, i.e. $\Omega^2 > 1/q^2$, another well known root is described by equation (1), which is the geodesic acoustic mode (GAM) with a frequency $\Omega^2 = 2(1+1/2q^2)$ [8–10]. The same branch was found in [11, 12] and [4], but was called the BAE branch.

Equation (1) is a cubic equation with regard to Ω^2, which is difficult to analyze with arbitrary coefficients. Instead, it was solved for the $k_0^2(\Omega^2)$ dependence near the resonance surface [1]. The solution describes the gap in the continuum and was shown to have the form

$$k_0^2 = \left[A^2 \pm \sqrt{A^4 - 16\delta\Omega^2 A(A-2)/q_r^2}\right] q_r^2/8, \tag{4}$$

where $A = \Omega^2 - q_r^2$. The graphical representation of this dispersion is shown in figure 1 and depends on poloidal and toroidal wave numbers via k_0. Figure 1 is useful in understanding the Alfvén–acoustic gap. It contains two solution, equations (2) and (3), for each value of

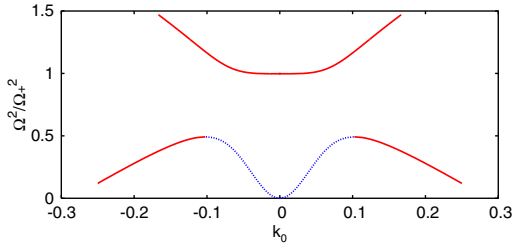

Figure 1. Solution of model dispersion relation as given by equation (4), in the high-m limit at $q_r = 1.75$ and $\delta = 2.5 \times 10^{-3}$. Plotted is the inverted dependence $k_0(\Omega^2)$. The frequency is normalized to the top gap frequency Ω_+^2, given by equation (5). The solid red line is the acoustic branch of the continuum, whereas the dashed blue line is the modified Alfvénic branch.

$k_0^2 < \delta/q_r^2 \simeq 0.008$. These solutions are transformed into the acoustic sidebands $\Omega^2 = k_{\pm 1}^2$ at $k_0^2 > \delta/q_r^2$.

Expressions for the Alfvén–acoustic continuum gap boundaries were also found in [1] by analyzing equation (4). They correspond to points at which $\partial k_0^2/\partial\Omega^2 \to \infty$, that is where k_0^2 has double roots. One such case is $A = 0$, where

$$\Omega^2 = \Omega_+^2 = 1/q_r^2. \tag{5}$$

The second case corresponds to the lower boundary of the gap

$$\frac{\Omega_-^2}{\Omega_+^2} = 1 + 16\delta\left(C^{1/3} - \frac{d}{3C^{1/3}}\right), \tag{6}$$

where $C = d\sqrt{4d + 27b^2}/6\sqrt{3} - bd/2$, $b = 1/16\delta$ and $d = 2q_r^2/16\delta$ which is further reduced in the limit of $\delta \ll 1$ (practically at $\delta < 0.2\%$) to

$$\Omega_-^2 = \Omega_+^2[1 - (32q^2\delta)^{1/3}]. \tag{7}$$

As can be seen from figure 1 the gap width is on the order of the gap frequency.

At the rational surface the frequency of the two acoustic sideband branches is inside the gap as well as the frequency of the resonance between the modified Alfvén dominant harmonic mode and acoustic sideband, which is the lowest of two and can serve as a rough estimate for the center of the gap

$$k_0^2 = \frac{\delta(1+2q^2)}{q^2}\left(1 + \sqrt{\delta(1+2q^2)}\right)^{-2},$$

and the center of the gap is at

$$\Omega_0 = \Omega_+/\left(1 + \sqrt{\delta(1+2q^2)}\right). \tag{8}$$

So the approximate lower gap boundary is

$$\Omega_- = \Omega_0 - \Delta\Omega/2, \tag{9}$$

where $\Delta\Omega \simeq 2\Omega_+\sqrt{\delta(1+2q^2)} = 2\delta\sqrt{1+2q^2}/q$. We show different approximations for the BAAE gap boundaries in figure 2.

The comparison of different continuum analytical solutions presented here and by the NOVA code continuum obtained numerically from ideal MHD for a specific case of circular surface plasma, based on the JET plasma, was done in [1] and showed remarkable agreement.

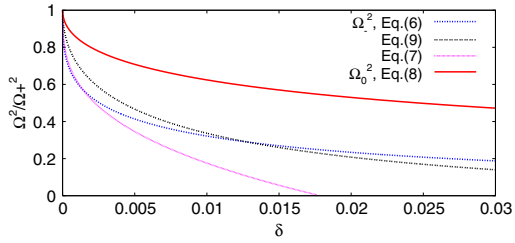

Figure 2. Comparison of the Alfvén/acoustic gap low boundary, Ω_-^2, following from different approximations (as indicated) of an exact solution of equation (6) versus the plasma beta parameter δ. Shown also is the frequency of the center of the gap, Ω_0^2. All frequencies are normalized to the upper boundary of the gap, Ω_+^2, given by equation (5).

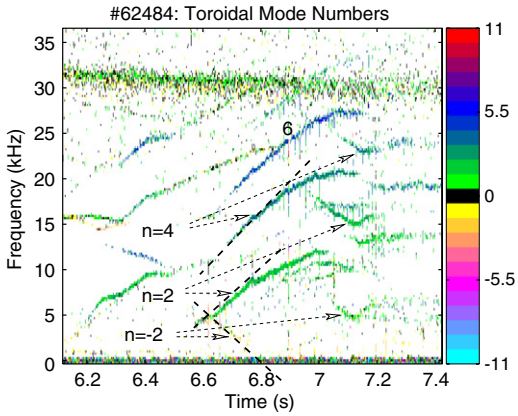

Figure 3. Magnetic signal frequency spectrum at the start of the discharge. Different colors represent different toroidal mode numbers corresponding to the color chart on the right. Black dashed lines are tangential to the signal initial evolution at $t = 6.6$ s.

3. Simulations and observations of BAAEs in low beta JET plasma

The measured spectrum of edge magnetic signal in JET, figure 3, shows low frequency signal evolution. One interesting and important observation is that only even mode numbers were observed $n = -2, 2, 4, 6$. The toroidal rotation has to be included in a further quantitative analysis, but was not measured in the experiment. It can be evaluated by comparing different ns, for example $n = -2$ and 2 signals at $t = 6.6$ s, i.e. when they are equal frequencies in the lab frame. Assuming that both modes have the same radial location, one can infer the rotation frequency $f_{\rm rot} \simeq 2$ kHz. The same value for $f_{\rm rot}$ emerges by comparing $n = -2$, 2 and 4 mode frequencies at $t = 7.1$ s.

This discharge was numerically analyzed in [1] using the NOVA code [13] under the assumption of the monotonic q-profile. For each n number two modes were found, one in the center at the low shear region and the other in the BAAE gap, near the top of the gap boundary. These are the locations where the continuum extrema points are formed (see also figure 1). In the low shear region the $\Omega(k_0)$ function is effectively stretched in the radial direction, which also creates a local continuum extremum (similar to RSAE formation [14, 15]). However, the main problem that previous JET simulations faced is the predicted BAAE frequency mismatch with the observations as we discussed in the introduction.

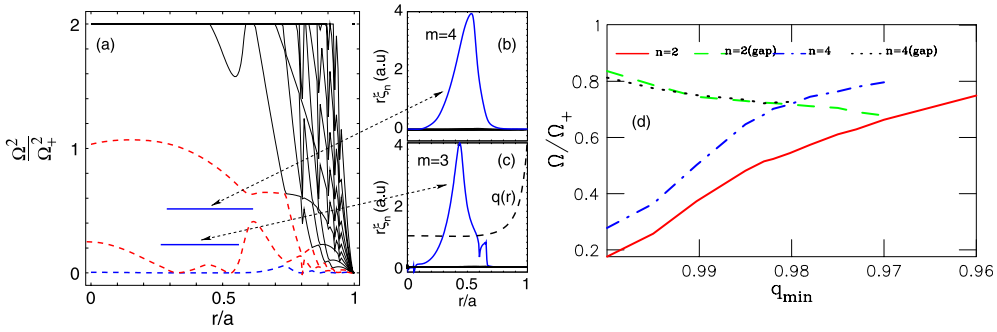

Figure 4. Alfvén–acoustic continuum (*a*) is shown as red dashed curves for the JET reversed magnetic shear plasma for $n = 4$ and $q_{\min} = 0.99$. The radial extents of the two global BAAEs and their frequencies are shown as solid lines near the extrema points. The radial mode structure of BAAE located in the gap is shown in (*b*) as the structure of its dominant poloidal harmonic of the normal component of the plasma displacement vector in arbitrary units. Figure (*c*) shows the radial structure of the low shear region localized BAAE along with the weakly reversed q-profile. Figure (*d*) shows BAAE eigenfrequencies as functions of $q_{\min}$ for the slightly reversed q-profile with $q_{\min}$ at $r/a = 0.45$. Frequencies are normalized to Ω_+, which corresponds to 31 kHz. Shown in (*d*) are localized mode frequencies at the low shear region, $n = 2$ (solid red curve) and $n = 2$ gap mode (dashed green curve), low shear $n = 4$ (blue dotted–dashed curve) and gap mode $n = 4$ (short dashed black curve).

Here in order to show the sensitivity of the BAAE frequency to the safety factor profile we study weakly reversed shear plasma with otherwise same plasma parameters as in [1]. The major radius is $R_0 = 2.90$ m, the minor radius is $a = 0.95m$, the magnetic field is $B_0 = 2.7$ T, the plasma beta profile is $\beta_{\rm pl} = \beta_{\rm pl0}[1 - (r/a)^2]^2\%$, $\beta_{\rm pl0} = 1\%$, the central electron density is $n_{\rm e0} = 1.3 \times 10^{13}$ cm^{-3}, the safety factor profile is taken in the form described in [16] with edge value $q_1 = 4$, $q' = {\rm d}q/{\rm d}\Psi$ equal to -0.2 and 30 at the center and at the edge, respectively, so that $q_{\min}$ is at $r/a = 0.45$ (for example, if $q_{\min} = 0.99$ then at the center $q_0 = 1.012$), $r/a \equiv \sqrt{\Psi}$ and Ψ is the normalized poloidal flux, last closed magnetic surface ellipticity 1.7 and triangularity 0.23. Plasma pressure is assumed to have only electron contribution. Simulations suggest that to find global BAAEs we need to assume a fairly extended region of the low shear region near the $q_{\min}$ surface. The plasma beta profile was fitted to measurements of the electron temperature and density, $T_{\rm e0} = 6$ keV. These plasma parameters correspond to the initial phase of JET discharge #62484, in which strong $\sim$2 MW ICRH was ramped up from $t = 5$ s. BAAE instabilities may have been driven by interaction with H-minority energetic components of the plasma, which are argued to excite the fishbones under similar plasma conditions [17].

We have found two global BAAEs, which are shown in figure 4 for $q_{\min} = 0.99$. As $q_{\min}$ is expected to decrease in time (due to plasma current diffusion) the Alfvén–acoustic continuum evolves and so do the frequencies of BAAEs according to figure 4(*d*). The reversed shear plasma results are qualitatively similar to the results with the monotonic shear profile [1]. For example, the low shear localized mode frequency is limited by the lower gap frequency, Ω_-, and starts from a small value. Numerically modes are not found near the lower extremum point inside the gap. This effect may be similar to the TAE frequency downshift effect due to the pressure gradient (eventually merging into the continuum near the gap) [18, 19].

In general BAAEs are robustly computed for both flat and slightly reversed q-profiles. In accordance with the developed theory in [1] we found that BAAEs contain one dominant poloidal harmonic, m, of radial plasma displacement and two sidebands $m \pm 1$ of the divergence

of plasma displacement vector with about equal amplitudes. This turned out to be similar to the behavior of recently reported observed modes in ASDEX and calculated with the CASTOR code in [20], where they were called low frequency cascade modes. These modes could also be BAAEs, but a detailed study of their properties is required in order to identify them as BAAEs.

The lowest value for BAAEs frequency is obtained if $\gamma = 1$, that is to use only electron beta for plasma equilibrium, $\beta_{\mathrm{pl}0} = \beta_{\mathrm{e}0} = 0.5\%$. This assumption seems to be consistent with the experimental conditions of strong H-minority heating and low plasma density, which means that ICRH power is primarily dumped into the electrons. Another indication of small ion temperature is a much weaker neutron signal at the beginning of the discharge than at its flattop, at which point the temperatures were measured to be comparable. In the case of low ion temperature, we find that Ω_+ corresponds to $f = 31.7$ kHz, which means that at the frequency crossing point of the low shear and gap BAAEs, $n = 4$ BAAE frequency is $0.7\Omega_+ \simeq 22$ kHz. Again, like in [1] this value is above the measured frequency $f_{n=4} = 14$ kHz by 1.57 (compare with the 1.77 factor for the monotonic q-profile [1]).

A rather simple suggestion to resolve the frequency mismatch in JET is to assume the existence of a local low (and reversed) shear region with $q_{\min} = 1.5$. In that case $\Omega_+ \simeq 21$ kHz, so that the monotonic q-profile would result in BAAE frequency ∼16 kHz, which is sufficiently close to observations. This conjecture would also solve the problem of observations of only even toroidal mode numbers, since $m = q_{\min} n$ must be integer. We have to note that at $t = 7$ s sawteeth-like events have been seen by soft x-ray measurements of electron temperature. There are indications that $q_0 \simeq 1$. This can still be consistent with the existence of local $q_{min} = 1.5$ at some radii away from the plasma center. More experiments are required in order to validate theoretical predictions for BAAE frequency.

Finally, a kinetic treatment of the eigenmode problem and/or finding an appropriate expression for γ is needed. One effect of kinetic theory is the drift frequency contribution, which turns out to be negligible. Indeed our estimates show that for $n = 4$ the drift frequency calculated with the pressure gradient is $\omega_{*\mathrm{pi}}/\omega_+ = 1.7 \times 10^{-2}$. Thus we conclude that the possible explanation for the observed magnetic activity based on drift instabilities fails [11,12]. However, another effect due to the non-perturbative role of energetic particles may be the reason for the mismatch of the computed and measured mode frequencies [21].

4. Observations of BAAEs in high beta NSTX plasma

Our theory predicts that at high plasma beta Alfvén and acoustic modes will be strongly coupled as δ becomes finite. Thus, it is important to explore high-β plasmas which are typical for spherical tokamaks. In addition the safety factor profile measurements with the motion Stark effect (MSE) diagnostic in NSTX make such a study very important for the quantitative validation of the theoretical predictions. A special experiment has been designed to verify the theory predictions and to attempt to reconcile the theory–experiment discrepancy obtained in the JET analysis presented in the previous section and in [1].

Similar conditions as in NSTX shot #115731 (described in [1]) were reproduced with more internal diagnostics applied for the purpose of mode identification. The following plasma parameters were achieved (at $t = 0.26$ s of the discharge): $R_0 = 0.855$ m, $a = 0.66$ m, safety factor as in figure 8(*a*), $\beta_{\mathrm{pl}0} \equiv 2\pi p(0)/B_0^2 = 0.34$, vacuum magnetic field at the geometrical center $B_0 = 0.44$ T, edge safety factor of $q_1 \simeq 13.86$, $q_0 \simeq 2.1$ and the same $\gamma = 1.375$, which is consistent with the TRANSP modeling, i.e. $T_{\mathrm{i}} \simeq T_{\mathrm{e}}$, and follows from kinetic theory [22].

NSTX magnetic activity spectrum evolution is shown in figure 5. This figure shows typical NSTX magnetic activity at the beginning of the discharge. First, RSAEs are observed with sweeping frequencies up and down, which however has an overall upward trend as the plasma

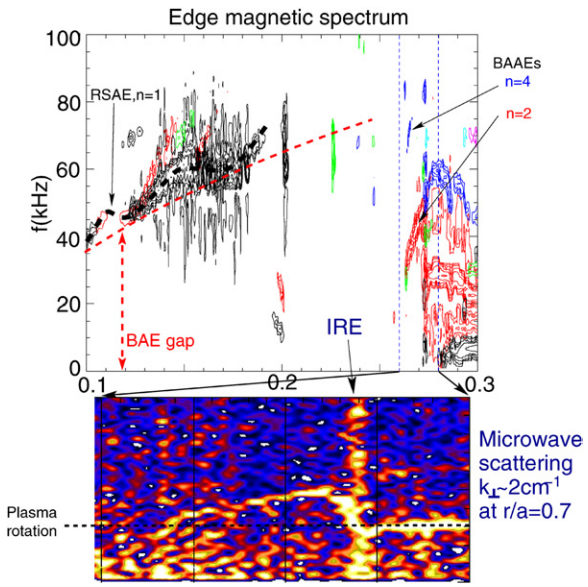

Figure 5. Magnetic activity spectrum evolution in NSTX discharge #123816 dedicated to BAAE study and shown for the $t = 0.1$–0.3 s time range. Various identified activities are indicated such as $n = 1$ RSAE and $n = 2, 4$ BAAEs. The lower color figure corresponds to the blown up time period of BAAE activity (vertical axis is the same) and is measured by the high-k scattering system, which diagnoses the plasma displacement with a specific range up to radial wavevectors $k_r \simeq 12\,\mathrm{cm}^{-1}$ at $R \simeq 1.45$ m (or $r/a \simeq 0.7$).

beta is accumulated and thus TAE/RSAE frequencies are up-shifted by the expanding BAE gap, the effect discussed theoretically in [4, 9, 18, 19, 23] and recently experimentally in [24]. After the total beta reaches a value of approximately 20% RSAE/TAE activity is suppressed, likely due to expected mode frequency moving into the continuum at high pressure gradients. Instead a lower frequency activity is often observed, such as marked BAAEs.

Figure 5 shows $n = 2, 4$ activity with frequencies from the level of plasma rotation ($f_{\mathrm{rot}} \simeq 15$ kHz) at $q_{\min}$ surface to about 50 kHz (for $n = 2$ mode) in the lab frame. From the microwave measurements inset of that figure one can notice that at $t = 0.275$ s some kind of internal reconnection event (IRE) happens as noted. After IRE the BAAE frequency goes down to the level of plasma rotation frequency, as indicated. This may indicate that the $q_{\min}$ value is changed back to its value at $t = 0.262$ s. Another interesting observation is that like in the JET plasma only even n-number BAAEs have been observed at $t = 0.262$–0.275 s.

The MSE diagnostic measured the q-profile, the results of which are shown in figure 6 in the form of $q_{\min}$ evolution. We compare the q_{min} MSE results with the values inferred from RSAE and BAAE observations (see figure 5). Times when the spectrum of $n = 1$ RSAE magnetic activity approaches the envelope of the upper BAE gap (GAM frequency, shown as a dashed curve in figure 5) serve as an indication of the rational value of $q_{\min}$. Such points are denoted as RSAE points in figure 6. As it follows from our theory, BAAEs with minimum frequency are expected to be observed at rational values of $q_{\min}$. From MSE and BAAE observations we infer that $q_{\min} = 3/2$ at $t = 0.262$ s. Note that this value is also consistent with the even n-numbers observations, that is $m = q_{\min} n$ must be integer.

We perform the NOVA numerical analysis for the plasma of interest by scanning $q_{\min}$. The MHD continuum for $q_{\min} = 1.43$ and $n = 2$ is shown in figure 7(a), which also shows

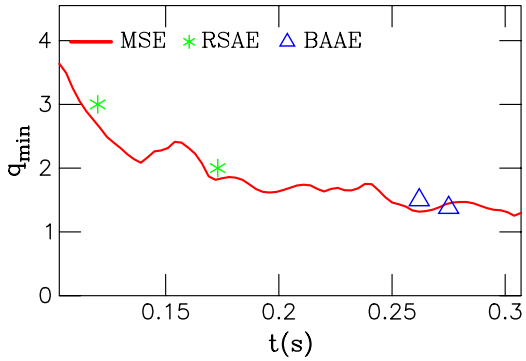

Figure 6. MSE measured evolution of $q_{\min}$ in the times of interest. Shown also are results of the comparison of the MHD RSAE and BAAE activities with the theoretical expectations for $q_{\min}$ values.

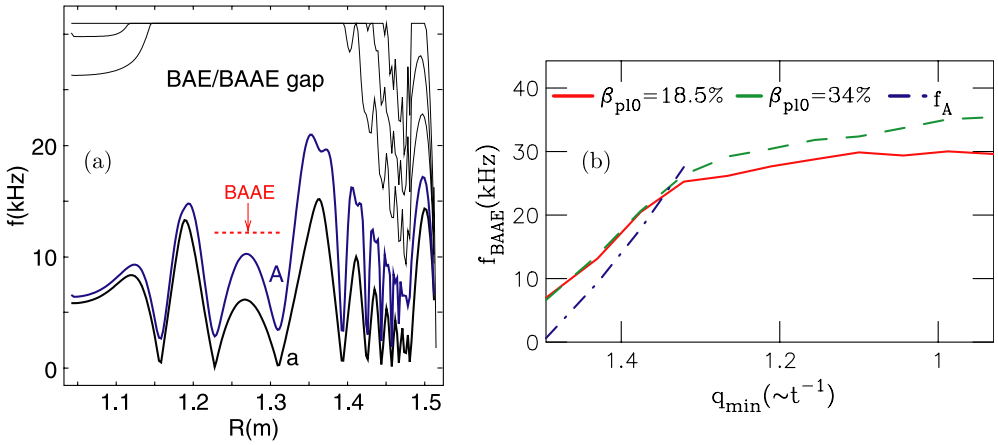

Figure 7. Shown in (*a*) are numerically simulated Alfvén–acoustic continuum and the position of BAAE (dashed horizontal line) for $n = 2$ and $q_{\min} = 1.43$. Indicated are the acoustic part (curve a) and the Alfvén part (curve A) of the continuum. Shown in (*b*) are frequencies of global BAAE modes as their frequencies sweep up versus $q_{\min}$ (approximately inversely proportional to time). We show BAAE eigenfrequency evolution for two plasma betas as indicated. Also shown is the expected modified Alfvénic branch continuum frequency, equation (3).

the radial extent and the frequency of the low shear global BAAE. Due to typically large beta of the plasma in NSTX the BAAE gap becomes large and merges with an otherwise wider BAE gap (we indicate them as one BAE/BAAE gap). However, like in JET, plasma continuum branches frequencies are still close to their cylindrical dispersion relations, indicated as A- and a-curves in figure 7(*a*). The global low-shear BAAE eigenfrequency follows closely the modified Alfvén continuum.

Numerically, we have found several global BAAEs for each $q_{\min}$ value in the scan. Shown in figure 7(*b*) are the BAAE eigenfrequency dependences for two plasma betas, $\beta_{pl0} = 18.5\%$ and $\beta_{pl0} = 34\%$. The shown frequencies correspond to solutions closest in frequency either to the continuum (low shear mode) with no radial nodes for $q_{\min} = 1.5$–1.35 or to the gap modes for $q_{\min} = 1.35$–0.85. Note that such a transition from low shear to the gap mode is continuous in NSTX, whereas in JET the low shear sweeping frequency solution is separated in frequency

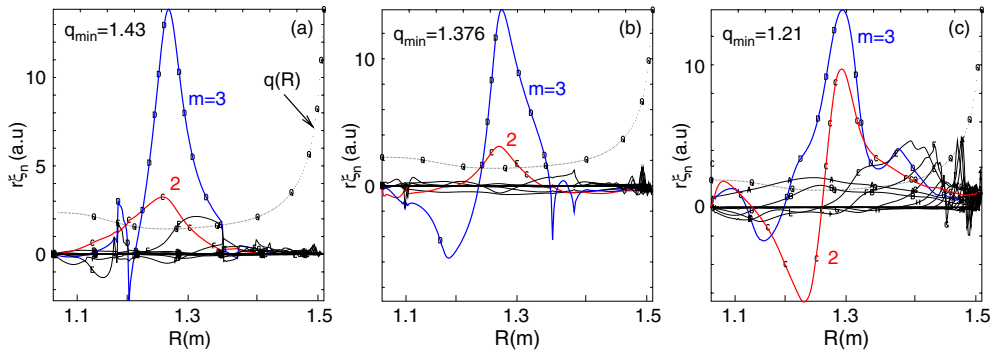

Figure 8. BAAE radial structures as computed by the NOVA code for different values of $q_{\min}$, as indicated. Shown in figures is the used reversed shear q-profile as was measured by MSE diagnostics.

from the gap solution as q decreases. This seems to be due to higher beta in NSTX. As one can see the absolute value of the BAAE frequency at the maximum of its frequency sweep in observations, i.e. 20 kHz (corrected for the Doppler shift from 50 kHz in the lab frame at $q_{\min} = 1.38$, $t = 0.274$ s), does not reach the value of the gap BAAE frequency. We show this point as the second BAAE point in figure 6, which seems to predict $q_{\min}$ in reasonable agreement with MSE measurements.

Since BAAE is bounded radially by the mth poloidal harmonic continuum we expected it to be radially strongly localized near the $q_{\min}$ radius when the BAAE frequency is at the bottom (near zero) of its sweep, that is when $q_{\min}$ is close to the rational value. As $q_{\min}$ decreases BAAE should broaden radially. Eventually, after entering the BAAE gap the mode structure is expected to be wide. This is similar to RSAE to TAE transition observed in DIII-D [25]. NOVA simulations support this as shown in figures 8(*a*)–(*c*), where radial dependences of the poloidal harmonics of the BAAE plasma displacement normal to the surface component (in the form $r\xi_n(r)$) are presented. Figure 8(*b*) corresponds to $q_{\min} = 1.376$, which is the second BAAE point in figure 6, $t = 0.274$ s. At that point BAAE is bounded by the continuum on the right, i.e. at $R = 1.35$ m, so that the mode structure seems to be broadened towards the center.

We compare these theory predictions with the internal fluctuation structure measured by the ultra-soft x-ray (USXR) fast camera diagnostic installed on NSTX. The USXR diagnostic records the x-ray emission integrated over the chords. Due to a strong gradient of the x-ray emission as a first approximation of the mode structure one can take the actual signal for the radial structure of BAAE without using a sophisticated inversion technique [26]. The evolution of the USXR radial mode structure shown in figures 9(*a*) and (*b*) is remarkably close to the theory predictions. Both the peak of the mode amplitude and its width are apparently similar to BAAE structures shown in figures 8(*a*) and (*b*). As we noted the BAAE does not seem to enter into the BAAE gap completely before possible IRE happens at $t = 0.275$ s.

Finally we make a comparison of the BAAE predicted radial displacement structure measured by the microwave reflectometer (local displacement). In each of the three discharges three point measurements were taken. These discharges had different plasma densities, which allowed the change in the location of the reflectometer points from plasma to plasma. The results and their comparison with NOVA predictions are shown in figure 10. The vertical axis corresponds to absolute data values for the plasma reported earlier, shot #123816, shown as solid, red circles. Each set of three points of other two plasmas was normalized in such a way that the first point (the smallest R value) lie on the theoretical curve. The comparison shows

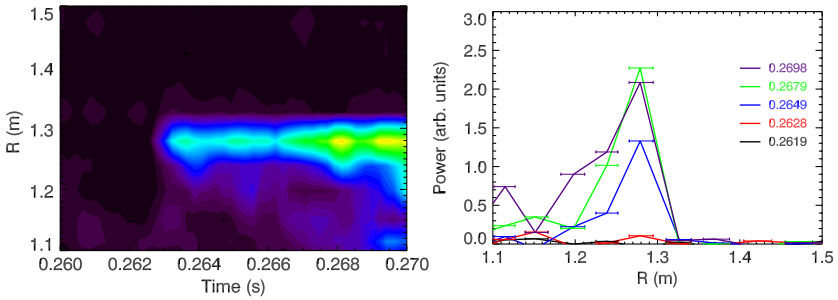

Figure 9. Raw USXR signal temporal behavior shown as a contour map in the plane t, R (a). Shown in (b) is the major radius dependence of the USXR signal taken at different times over the BAAE frequency sweep, as indicated.

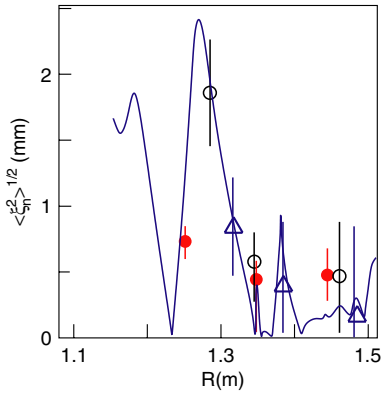

Figure 10. Comparison of the NOVA predicted RMS value of the normal component of the plasma displacement with the reflectometer measurements for #123816 NSTX shot at $t = 0.27$ s and $n = 2$.

that reflectometer data are in qualitative agreement with NOVA predictions for the BAAE localization. The maximum absolute radial plasma displacement and density perturbation measured by the reflectometer were about $\xi_r/a \sim 10^{-3}$ and $\delta n/n \sim 3 \times 10^{-3}$, respectively.

Note that because NOVA is the ideal MHD code, it cannot be relied upon for the prediction of the localized mode behavior beyond the point of its interaction with the continuum. In the case of the gap mode, figure 8(c), it is $R > 1.4$ m. At that location the mode conversion is expected from BAAE to kinetic Alfvén wave solution (KAW) and at which point high-k measurements were done as presented in figure 5. The measured range of radial wavevectors is around $k_\perp \simeq 2\,\mathrm{cm}^{-1}$. A longer wavelength channel picks up a weaker BAAE signal, which indicates the presence of the conversion layer. Similar observations have been made for the TAE to KAW conversion on TFTR [27].

5. Summary and discussion

In this paper we presented a theoretical description of the ideal MHD Alfvén–acoustic continuum gap in the limit of a low beta and high aspect ratio plasma. Numerically we have found new global eigenmodes, called here BAAEs, which are formed near the extrema points of the continuum in both low and high beta plasmas. We also presented

experimental observations, which qualitatively and quantitatively support our theoretical predictions.

In previous work [1] and in this paper we found that ideal MHD simulated BAAE frequency evolution qualitatively agrees with JET observations. However the analysis of the monotonic q-profile plasma suggests that at the point when the BAAE frequency enters the Alfvén–acoustic its frequency is higher by a factor of 1.77 [1] (1.57 in the case of the reversed shear profile model in this paper) than the highest frequency observed for these modes. This is the lowest value ideal MHD can provide by keeping only thermal electron (neglecting bulk ion) pressure. The model for γ as well as kinetic effects such as those due to thermal ion FLR and non-perturbative interaction with energetic particles [21] may also be responsible for the mismatch in computed and measured mode frequencies.

In this paper we point out another potential way to reconciling simulations and observations in JET, which is to assume that in the plasma there is a region with local $q_{\min} = 1.5$, in which case localized BAAEs with only even toroidal mode numbers can exist ($m = q_{\min} n$ must be integer) and the gap BAAE eigenfrequency is 1.5 times lower in simulations. This would bring NOVA predictions for the BAAE frequency within reasonable uncertainty of 10% to the observed $f = 14\,\mathrm{kHz}$. Therefore, the EFIT equilibrium solver prediction that q_0 is close to unity and other observations, such as sawtooth like events about 1 s after BAAE observations, challenges theory. This may be resolved by more detailed measurements of the q-profile. The required current drive profile modification can be due to several effects, such as off-axis ICRH induced current drive and radial transport (and current drive redistribution) of H-minority ions due to MHD activity, such as present TAEs and BAAEs. Finally, in such low density of the plasma a substantial part of the current can be carried by the runaway electrons [28].

The study of the q-profile by the MSE diagnostic was in the center of the recent NSTX experiments reported here where BAAEs were observed. Indeed, even $n = 2, 4$ modes with sweeping frequencies have been observed at the same time when $q_{\min}$ was close to the $3/2$ value. Detailed measurements of the BAAE internal structure revealed the same radial localization, eigenfrequency and their evolution as was predicted by theory. We note that the reported BAAEs in NSTX seem to stay near the modified Alfvén continuum frequency and do not enter the Alfvén–acoustic gap. BAAEs are typical for NSTX high beta plasma and strong beam ion population. A strong drive is required in NSTX where electron and ion temperatures are similar so that strong ion Landau damping is also expected, which is likely due to acoustic mode coupling. However, if both the drive and the damping are strong one can expect that BAAEs open a potential energy channeling from beam ions directly to thermal ions without going first to the electrons. This is similar to the idea of α-channeling suggested for tokamaks [29].

The stability of BAAEs is beyond the scope of this paper and requires kinetic treatment.

The frequency of sweeping up the BAAE mode can be used to determine the q_0 value, in particular in high-β NSTX plasmas, where RSAE/TAEs seem to be stabilized by strong interaction with the continuum. Values of q_0 determined this way were compared with the MSE measurements and were found to be in agreement. Such an extension of MHD spectroscopy could be of great importance to ITER and other burning plasma devices. Potentially BAAE observations can provide additional constraints for the values of ion and electron temperatures.

Finally we note that the frequency of BAAE is lower than the frequency of the GAM (BAE) [30, 31, 7] frequency by a factor of $\sqrt{2(q^2+1)}$, but both scale in a similar way with the plasma parameters. This property can be used to separate two instabilities in experiments, which is especially true for high $q_{\min}$ plasmas. An additional character of BAAEs is that they can sweep in frequency, which is opposite to BAE with persistent frequency, changing on a much longer time scale [30].

Acknowledgments

This work was supported in part by the US Department of Energy under the contracts DE-AC02-76CH03073 and DE-FG03-96ER-54346 and in part by the European Fusion Development Agreement.

References

[1] Gorelenkov N N, Berk H L, Fredrickson E and Sharapov S E 2007 *Phys. Lett.* A **370** 70–7
[2] Gorelenkov N N, Berk H L and Fredrickson E D 2006 *Bull. Am. Phys. Soc.* **51** 183 (abstract NO1 10)
[3] Goedbloed J P 1975 *Phys. Fluids* **18** 1258
[4] Chu M S, Greene J M, Lao L L, Turnbull A D and Chance M S 1992 *Phys. Fluids* B **11** 3713
[5] Goedbloed J P 1998 *Phys. Plasmas* **5** 3143
[6] van der Holst B, Beliën A J C and Goedbloed J P 2000 *Phys. Plasmas* **7** 4208
[7] Huysmans G T A, Kerner W, Borba D, Holties H A and Goedbloed J P 1995 *Phys. Plasmas* **2** 1605
[8] Winsor N, Johnson J L and Dawson J M 1968 *Phys. Fluids* **11** 2448
[9] Breizman B N, Sharapov S E and Pekker M S 2005 *Phys. Plasmas* **12** 112506
[10] Berk H L, Boswell C J, Borba D N, Figueiredo A C A, Johnson T, Nave M F F, Pinches S D and Sharapov S E 2006 *Nucl. Fusion* **46** S888
[11] Zonca F, Chen L and Santoro R 1996 *Plasma Phys. Control. Fusion* **38** 2011
[12] Mikhailovskii A B and Sharapov S E 1999 *Plasma Phys. Rep* **25** 838
[13] Cheng C Z and Chance M S 1986*Phys. Fluids* **29** 3695
[14] Breizman B N, Berk H L, Pekker M S, Pinches S D and Sharapov S E 2003 *Phys. Plasmas* **10** 3649
[15] Sharapov S E, Mikhailovskii A B and Huysmans G T A 2004 *Phys. Plasmas* **11** 2286
[16] Cheng C Z 1992 *Phys. Rep.* **211** 1
[17] Nabais F, Borba D, Mantsinen M, Nave M F F and Sharapov S E 2005 *Phys. Plasmas* **12** 102509
[18] Fu G Y and Berk H L 2006 *Phys. Plasmas* **13** 052502
[19] Gorelenkov N, Kramer G and Nazikian R 2006 *Plasma Phys. Control. Fusion* **48** 1255
[20] Lauber P, Günter S, Brüdgam M, Könies A and Pinches S D 2006 *AIP Conf. Proc.* **871** 147
[21] Gorelenkov N N and Heidbrink W W 2002 *Nucl. Fusion* **42** 150
[22] Mazur V A and Mikhailovskii A B 1977 *Nucl. Fusion* **17** 193
[23] Kramer G J, Gorelenkov N N, Nazikian R and Cheng C Z 2004 *Plasma Phys. Control. Fusion* **46** L23
[24] Fredrickson E D, Crocker N A, Gorelenkov N N, Heidbrink W W, Kubota S, Levinton F M, Yuh H, Menard J E and Bell R E 2007 *Phys. Plasmas* **14** submitted
[25] Zeeland M A V, Kramer G J, Austin M E, Boivin R L, Heidbrin W W, Makowski M A, McKee G R, Nazikian R, Solomon W M and Wang G 2006 *Phys. Rev. Lett.* **97** 135001
[26] Fredrickson E D *et al* 2006 *Phys. Plasmas* **13** 056109
[27] Wong K L, Bretz N, Fu G Y, Machuzak J, Wilson J R, Chang Z, Chen L, Owens D K and Schilling G 1996 *Phys. Lett.* A **224** 99
[28] Sandquist P, Sharapov S E, Helander P and Lisak M 2006 *Phys. Plasmas* **13** 072108
[29] Fisch N J and Rax J-M 1992 *Phys. Rev. Lett.* **69** 612
[30] Heidbrink W W, Strait E J, Chu M S and Turnbull A D 1993 *Phys. Rev. Lett.* **71** 855
[31] Turnbull A D, Strait E J, Heidbrink W W, Chu M S, Duong H H, Greene J M, Lao L L, Taylor T S and Thompson S J 1993 *Phys. Fluids* B **5** 2546

The Princeton Plasma Physics Laboratory is operated
by Princeton University under contract
with the U.S. Department of Energy.

Information Services
Princeton Plasma Physics Laboratory
P.O. Box 451
Princeton, NJ 08543

Phone: 609-243-2750
Fax: 609-243-2751
e-mail: pppl_info@pppl.gov
Internet Address: http://www.pppl.gov